J.Natn.Sci.Foundation Sri Lanka 2022 50 (4): 839 - 850
DOI: http://dx.doi.org/10.4038/jnsfsr.v50i4.10586

RESEARCH ARTICLE

Corrosion

Developing a model to predict the propagation of sulphide stress corrosion of steel used for petroleum pipelines

A Manimendra[1*], I De Silva[1] and R Jayasundara[2]
[1] *Department of Materials Science and Engineering, Faculty of Engineering, University of Moratuwa, Sri Lanka.*
[2] *Department of Mathematics, Faculty of Engineering, University of Moratuwa, Sri Lanka.*

Submitted: 17 June 2021: Revised: 05 August 2022: Accepted: 26 August 2022

Abstract: Sulphide stress corrosion (SSC) is an abundant type of corrosion in petroleum refineries. Steel pipes in petroleum refineries are influenced by the synergistic effect of tensile stress/pressure and high H_2S concentrations in different environments. This paper focuses on the prediction of the propagation of depth of SSC in API 5L Grade B steel as a function of pH value, applied load, and time duration. The model has been established based on the experimental values of the depth of SSC under different predetermined test environmental conditions kept within the pH value of 2.7–3.5, an applied load of 400–800 N, and a time duration of 15–45 days. Further, the model was validated by another data set obtained for the depth of corrosion within the same aforementioned ranges of parameters. All the laboratory experiments were conducted in accordance with ANSI/NACE TM0177-2016 standard test methods. In addition, this paper discusses the microstructural observations of specimens kept under the aforementioned test environmental conditions. The scanning electron microscope (SEM) images of cross-sections of corroded specimens showed that crack initiation occurred after 15 days under all different test environmental conditions. Further, crack propagation occurred transversely, developing branches through the cross section until 30 days of time duration and the behaviour of the propagation of the crack was completely changed at 45 days of time duration.

Keywords: API 5L grade B steel, depth of corrosion, mackinawite, sulphide stress corrosion, sulphur.

INTRODUCTION

Corrosion is one of the main phenomena considered in engineering design because most of the failures in power plants, infrastructure constructions, and machinery occur due to the effect of corrosion (Foroulis, 1996; European Commission, 2013). Sulphide stress corrosion (SSC) predominantly occurs in petroleum power plants due to the synergistic effect of pressure/tensile force exerted on components and their corrosive environment containing H_2S. Petroleum pipelines can be identified as one of those components that are severely attacked by sulphide stress corrosion as they are exposed to extreme pressure conditions with high H_2S concentrations (Gosette, 2007; Pieris *et al*., 2020).

Sulphide stress corrosion must be carefully controlled as it causes failures without a prior warning. Techniques such as non-destructive testing (NDT), SEM image analysis, optical techniques, and electrochemical techniques are applied to time-based inspection routines to track the sulphide stress corrosion. They indicate only the extent to which the corrosion has propagated. If the corrosion mechanism behaves in an unexpected way in between two inspections, there is a possibility of failure in pipelines, which would have an adverse impact on the industry. Therefore, the petroleum industry focuses on developing mathematical and statistical prediction models to get accurate predictions for the propagation of sulphide stress corrosion.

Even though prediction models have been developed over the past fifteen years to predict the propagation of SSC, some of them are not very accurate (Traidia, 2018). The rest of the models make accurate predictions under

* Corresponding author (akeshmanimendra@gmail.com; https://orcid.org/0000-0002-4684-6621)

certain conditions. It can be seen that the results predicted by the model developed by Asmara *et al.* (2013) deviated significantly from the experimental values when the time period was increased beyond 800 hours. Some of the models predict accurate results when they are predicting corrosion behaviour at low H_2S concentrations (Sun & Nesic, 2007), while some of the other models predict accurate results at high H_2S concentrations (Asmara *et al*., 2013). SSC-based research has been conducted for the materials which are used to manufacture oil country tubular goods (OCTG). Some of the common materials that have been used for sulphide stress corrosion-based experiments are API 5L grade B steel, AISI 4137H steel, AISI 1018 carbon steel, 20# steel, X65 pipeline steel, FV520B steel etc. (Asahi *et al*., 1994; Smith *et al*., 2002; Sun & Nesic, 2007; Liao *et al*., 2012; Zheng *et al*., 2014). All these metals used in OCTG are mild steel types. The present study focuses on predicting the propagation of sulphide stress corrosion of API 5L grade B steel that is used for manufacturing the pipes used in the refinery system of the Ceylon Petroleum Corporation. Furthermore, there is a possibility of applying this developed model to a part of this refinery system to ensure the functionality and accuracy of the model in a real working environment.

MATERIALS AND METHODS

Materials

API 5L Grade B steel samples, procured from Ceylon Petroleum Corporation in the form of a seamless pipe of 1 m in length, 11 mm in thickness and 168 mm in diameter, were used for the experiments. The chemical composition (Table 1) of the sample was verified by spark emission spectroscopy (Model: Ametek-spectrocheck). The maximum allowed weight fractions are given as per the API 5L 45th edition of the specification for line pipes (American Petroleum Institute, 2003).

Table 1: Chemical composition of API 5L grade B steel

Element	Mass fraction (%)	Max allowed weight fraction (%)
Fe	98.600	Not specified
C	0.201	0.28
Si	0.292	Not specified
Mn	0.470	1.20
P	0.029	0.03
S	0.007	0.03
Cr	0.059	0.50
Ni	0.103	0.50
Al	0.043	Not specified

Experimental setup – Test conditions in the corrosive vessel

Fabrication of the test vessel and specimens

Fabrication of the test vessel and test specimens were carried out in accordance with the ANSI/NACE TM0177-2016 standard test method. The test vessel was made out of 5 mm thick acrylic sheets, and the chamber was sealed by applying silica glue (Figure 1). The test vessel was tested for leaks with N_2 gas at 1.5 atm. The total volume of the test vessel was 2856 cm^{3,} while the volume of the test solution was 2000 cm^3 (70.0 % of the volume of the test vessel). The test specimen was prepared using the CNC machining technique since the specimens can be machined without overheating and cold working. The final surface finish was achieved through mechanical polishing that was done using 0.25 µm grit papers. The dimensions of the test specimen are shown in Figure 2.

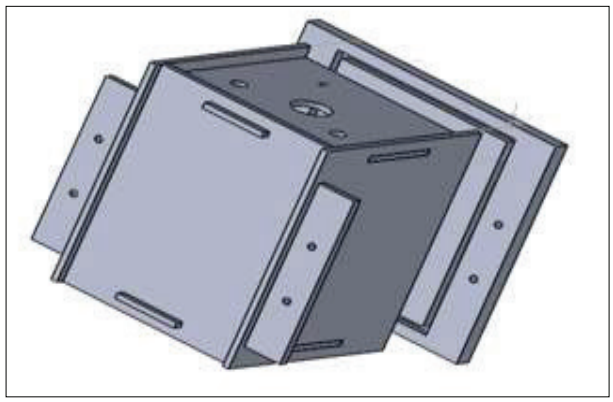

Figure 1: Designed model of the test vessel

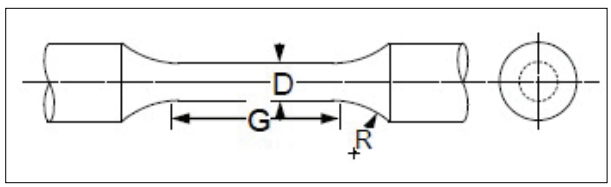

Figure 2: Dimensions of the test specimen
G = 55.00 mm, D = 6.72 mm, R = 1.00 mm

The sample holder was made out of mild steel, and it was fully coated with an epoxy coating to mitigate the influence of galvanic corrosion. The final experimental setup is shown in Figure 3.

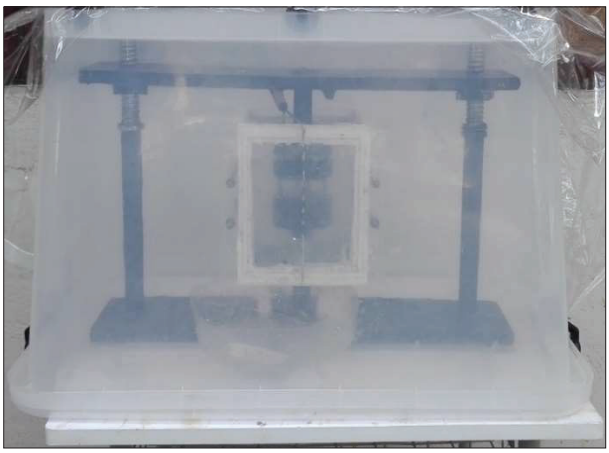

Figure 3: Experimental setup

Test conditions

The specimens were kept under 18 different test conditions/environments, which were predetermined by varying the applied load to the test specimen, the pH value of the H_2S solution, and time duration, as shown in Table 2. Three specimens were tested for each set of conditions. Temperature and pressure were maintained at 24 ± 3 ˚C and 1 atm, respectively.

Table 2: Test environmental conditions

No	Applied load (N)	pH value	Time duration (days)
1	400	2.7	15
2	600	2.7	15
3	800	2.7	15
4	400	3.5	15
5	600	3.5	15
6	800	3.5	15
7	400	2.7	30
8	600	2.7	30
9	800	2.7	30
10	400	3.5	30
11	600	3.5	30
12	800	3.5	30
13	400	2.7	45
14	600	2.7	45
15	800	2.7	45
16	400	3.5	45
17	600	3.5	45
18	800	3.5	45

The loads were applied to the specimen as a constant load in accordance with the Method A – standard tensile test mentioned in the ANSI/NACE TM0177-2016 standard test method (NACE International Standard, 2005). Test solutions A and B mentioned in the standard (NACE International Standard, 2005) were prepared to maintain the pH value at 2.7 and 3.5, respectively.

Determination of depth of corrosion by SEM observations

The specimens corroded under the 18 test conditions were prepared for SEM observations. Observations were performed by the SEM [Model: SEM- ZEISS EVO18-Research] under BSD mode with a 100 µA current. The magnification was determined based on the crack length. At the end of the specified time duration, each specimen was taken out of the test vessel and washed with DI water. Each test specimen was slashed transversely by using a low-speed precision cutting machine at three different places to obtain three different cross-sections (Figure 4).

Three different segments of each cross-section were observed by SEM, and the maximum depth of corrosion for each segment was identified. The depth of corrosion for a selected cross-section (d) was obtained by calculating the average value of three maximum depths of corrosion (Figure 4).

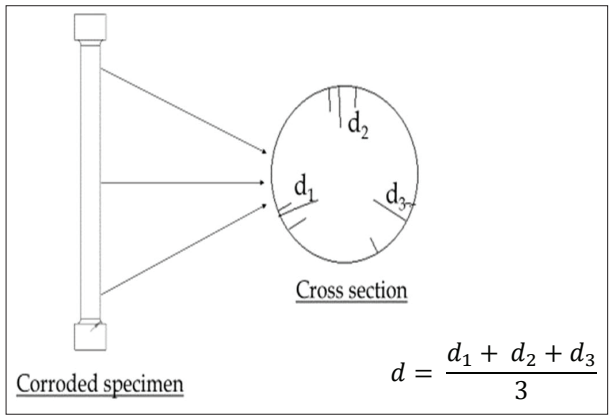

Figure 4: Three transverse cuts of a specimen and obtaining average depth of corrosion

Since there had been three cross-sections obtained for one specimen, the depth of sulphide stress corrosion of a selected specimen was obtained by calculating the average value of the depth of corrosion of each cross-section. Following that, the depth of sulphide stress

corrosion of the API 5L Grade B steel for a specific test condition was obtained by calculating the average of depth of corrosions of three specimens which were corroded under this specific test condition.

SEM/EDAX analysis of SSC cracks

The SCC cracks were further analysed using SEM/EDAX elemental line profiles. The distribution of sulphur within the crack surface was investigated using this technique.

Development of the statistical model

The statistical model was developed using experimental data to predict the depth of corrosion of the sulphide stress corrosion as a function of the time duration, pH value of the solution, and applied load. At the development stage of the model, a linear relationship, normality of responses, little or no multi-collinearity, no autocorrelation and homoscedasticity were assumed (Statics Solution, 2016). The depth of corrosion was considered the dependent variable of the model, while the time duration, pH value, and applied load were considered independent variables. Multiple linear regression analysis was selected over nonlinear regression analysis, as the model becomes simpler to use.

Validation of the model assumptions

1. Multiple linear regression needs the relationship between the independent and dependent variables to be linear. Therefore, the outliers were also checked since multiple linear regression is sensitive to outlier effects. Scatter plots were prepared for the testing of linearity. As the dependent variable was not linearly related to some independent variables, a nonlinear transformation was carried out.
2. As the multiple linear regression analysis requires residuals to be normal, this assumption was checked with a histogram and a *p-p* plot.
3. Multi-collinearity was checked against four key criteria mentioned below.

- Correlation matrix – when computing the matrix of Pearson's Bivariate Correlation among all independent variables, the correlation coefficients need to be smaller than 1.
- Tolerance – the tolerance measures the influence of one independent variable on all the other independent variables. Tolerance is defined as $T = 1 - R^2$ for these first-step regression analyses. With $T < 0.1$, there might be multi-collinearity in the data, and with $T < 0.01$, there certainly is.
- Variance Inflation Factor (VIF) – the variance inflation factor of the linear regression is defined as VIF = 1/T. Similarly, with VIF > 10, there is an indication for multi-collinearity to be present.
- Condition Index – the condition index was calculated using a factor analysis of the independent variables. Values of 10–30 indicate a mediocre multi-collinearity in the regression variables, and values > 30 indicate strong multi-collinearity

4. Multiple linear regression analysis requires that there is little or no autocorrelation in the data. Autocorrelation occurs when the residuals are not independent of each other. The Durbin-Watson test was carried out to check the autocorrelation.
5. Another assumption of multiple linear regression analysis is homoscedasticity. The scatter plot was used to check homoscedasticity.

RESULTS AND DISCUSSION

Implementation of the model

The developed statistical model predicts the depth of sulphide stress corrosion in terms of time duration, pH value, and applied load, as expressed in the following formula.

$$DoC = -5.035e^{pH} - \frac{95455.143}{Applied\ Load} + 4.333 \times 10^{-6} \times Time^{4.45} + 400.140 \quad ...(1)$$

Where,

DoC = the depth of sulphide stress corrosion in micrometres
Applied Load = the applied load on the test specimen in N
Time = the time duration in days that the specimen has been exposed to test environment
pH = average pH value of the test solution

The implemented empirical formula was subjected to a series of statistical tests to confirm if it satisfies the initial assumptions made.

Figure 5, Figure 6, and Table 3 stand for the normality test of the model. The histogram (Figure 5) shows a normal bell curve shape indicating that all standardized residuals are normally distributed in the model. The *p-p* plot (Figure 6) indicates that the expected cumulative probability vs observed cumulative probability plot lies along the normal line. The linear behaviour of the model

was further confirmed by Shapiro Wilk *p* values, which are shown in Table 3. It can be seen that the *p* values obtained for standardized residuals and unstandardized residuals are equal to each other. Further, based on the null hypothesis of H_0 – depth of corrosion is normally distributed in the population, and the alternative hypothesis of H_1 – depth of corrosion is not normally distributed in the population, at 5% significance level, since the asymptotic significance is greater than 5%, the null hypothesis is not rejected, and it can be concluded that the dependent variable is normally distributed in the population.

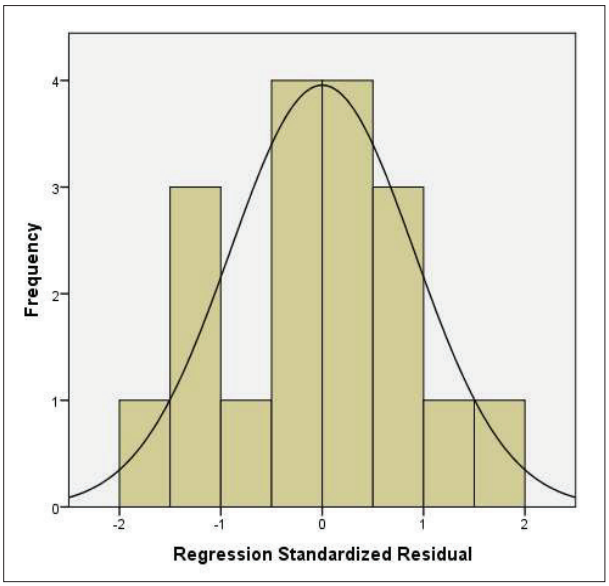

Figure 5: Histogram of frequency vs regression standardized residual

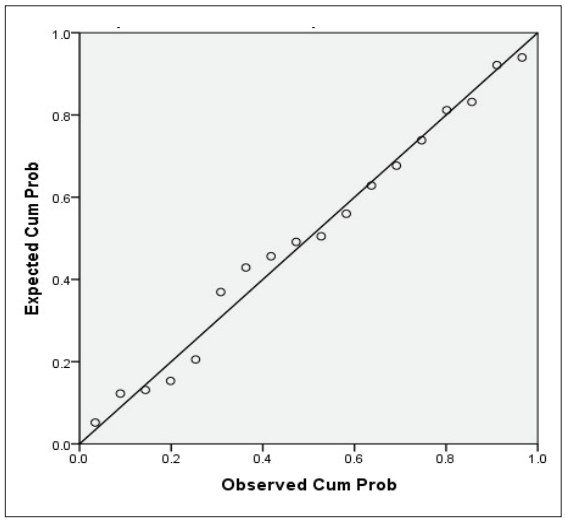

Figure 6: Normal *P-P* plot of regression standardized residuals

Table 3: Test of normality

	Shapiro-Wilk		
	Statistic	df	sig
Unstandardized residual	0.974	18	0.867
Standardized residual	0.974	18	0.867

Table 4 shows the Pearson's bivariate correlation matrix for the dependent variables and independent variables. It can be seen that all correlation coefficients are less than 0.08 other than the coefficient between time 0.455 and the depth of sulphide stress corrosion (Table 4).

Table 4: Pearson's correlation matrix

Variable	Depth of sulphide stress corrosion	e^{pH}	$Time^{4.45}$	1/Load
Depth of sulphide stress corrosion	1.000	-0.487	0.455	-0.526
e^{pH}	-0.487	1.000	0.000	0.000
$Time^{4.45}$	0.455	0.000	1.000	0.000
1/Load	-0.526	0.000	0.000	1.000

Therefore, it can be considered that the multi-collinearity in data is negligible. Variance inflation factor (VIF), tolerance, and condition index were tested for the multi-collinearity diagnostics, and tolerance values (Table 5) for all dimensions are 1 (>>> 0.1). It proves again that the multi-collinearity in data is negligible. Furthermore, VIF values and condition index values that were obtained for model dimensions indicate that they are less than 10 (Table 5). Therefore, these values provide evidence that no multi-collinearity is found in the data.

Table 5: Collinearity diagnostic tables

Model dimensions	Tolerance	VIF	Condition index
Constant	1.000	1.000	1.000
e^{pH}	1.000	1.000	2.661
1/Applied Load	1.000	1.000	5.690
$Time^{4.45}$	1.000	1.000	10.353

The autocorrelation was tested by the Durbin-Watson test, and the statistic says the value is 1.343. This indicates that the residuals are not linearly autocorrelated. Hence autocorrelation in the data is negligible.

The homoscedasticity of data was tested using scatter plots of standardized residuals vs standardized predicted values (Figure 7) and standardized residuals vs unstandardized predicted values (Figure 8). Both the scatter plots are rectangular enough to conclude the homoscedasticity in the data.

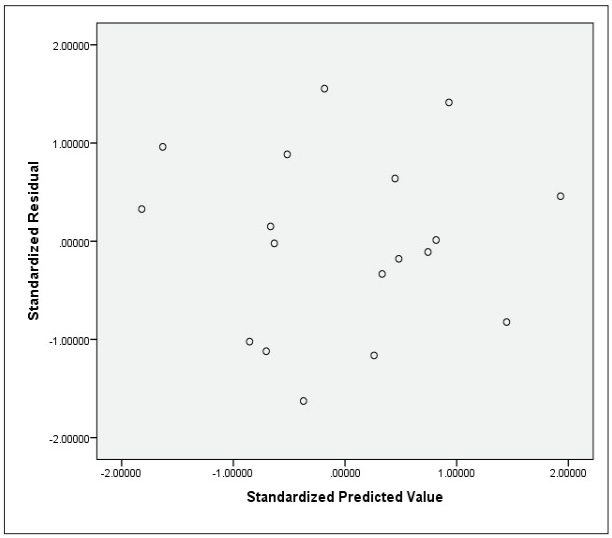

Figure 7: Scatter plot of standardized residuals vs standardized predicted values

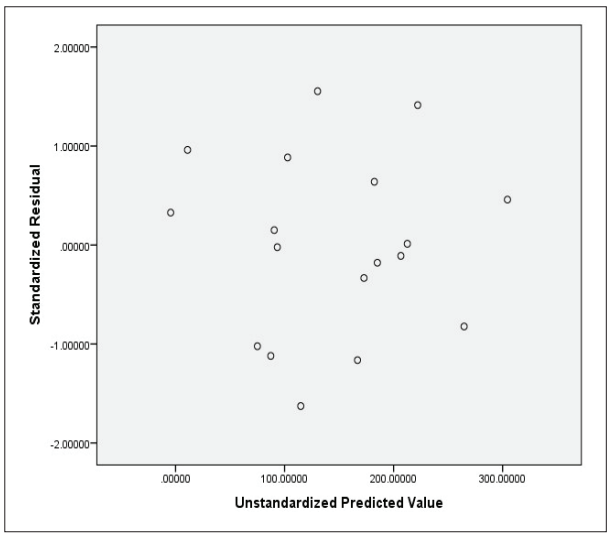

Figure 8: Scatter plot of standardized residuals vs unstandardized predicted values

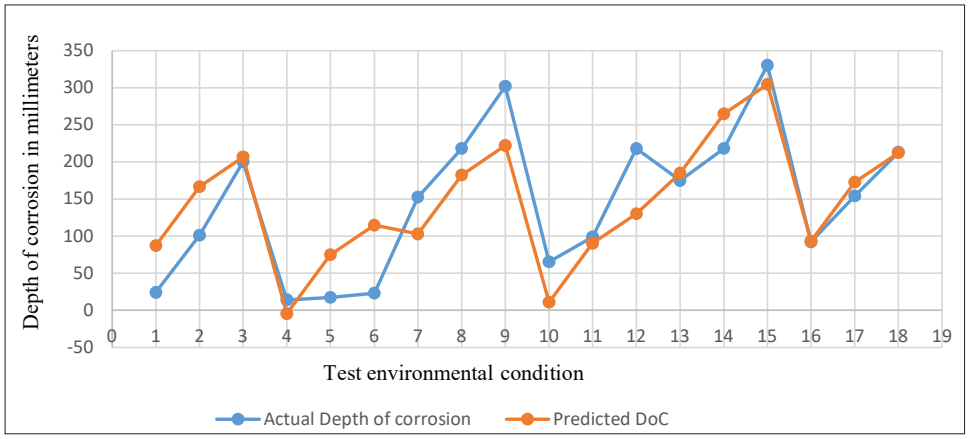

Figure 9: The comparison of model predicted values and experimental values of depth of sulphide stress corrosion at 27 ˚C and 1 atm under different test environmental conditions

Validation of the model based on the predetermined test environmental conditions

Model predictions were compared with the experimental values that were used to develop the model, as shown in Figure 9. The test environmental conditions given by Figure 9 correspond to the test environmental conditions defined in Table 2. The range of parameters considered are such that pH values vary between 2.7 and 3.5, applied loads vary between 400 N, 600 N, and 800 N, and time durations vary between 15 days, 30 days, and 45 days. All the depths of corrosions were between 24 μm and 214 μm.

It can be seen in Figure 9 that the depth of sulphide stress corrosion varies with the test environmental conditions in a manner similar to the behaviour of a wave. The variation of experimental values of depth of corrosion under different test environments agrees well with the values predicted by the model. It can be seen that the model successfully captures the upward and downward trends of the depth of sulphide stress corrosion with time duration, applied load, and pH value. From test environmental conditions 1 to 3, there can be seen an increase in the depth of corrosion. But the test environmental condition 4 shows a sudden reduction of the depth of sulphide stress corrosion. Again, an increase in the depth of sulphide stress corrosion can be observed from test conditions 4 to 6. If one set of depths of corrosion values which are monotonically increased, is identified as one cluster, three clusters can be seen up to the test environmental condition 10. Every cluster includes three depths of corrosion values obtained under the applied loads of 400 N, 600 N, and 800N each. However, the pH values and the time durations were constant within a certain cluster.

This behaviour is no longer obeyed from the 10th test environmental condition onwards. According to the previous pattern, test environmental condition 13 should have a smaller depth of corrosion value compared to the value shown at test environmental condition 12. Instead, the depth of corrosion values is monotonically increased from test environmental conditions 10 to 15. However, a reduction in the depth of corrosion at the 13th environmental condition was observed in the experimental depths of corrosion. The test environmental conditions 10 to 15 differ from test environmental conditions 1 to 10 mainly by time duration. The usual cluster pattern behaviour starts to be disobeyed at the 13th environmental condition when the time duration is 45 days. The cluster pattern behaviour occurring from the 15th test environmental condition onwards cannot be predicted properly, as experiments were continued only up to the 18th test environmental condition.

However, the errors occurred at (pH = 2.5, load = 400 N, Time = 15 days), (pH = 3.5, load = 400 N, Time = 15 days), (pH = 3.5, Load = 600 N, Time = 15 days) and (pH = 3.5, Load = 800 N, Time = 15 days) reflected an outlying nature. Accordingly, the average percentage error calculated disregarding the outlying points was -7.65%. Thus, the model was considered for predictions after model validation was done using five more experimental data values.

Validation of the model based on the random test environmental conditions

Model predictions were further compared with experimental results obtained under random test environmental conditions. The test environmental conditions were maintained within the two extremes of pH = 3.5, Applied load = 400 N, Time duration = 15 days and pH value = 2.7, Applied load = 800 N, Time duration = 45 days. Figure 10 shows the comparison between model prediction values and the experimental results obtained under random test environmental conditions. Table 6 shows the corresponding test environmental conditions, maintained at a temperature of 24 ± 4 °C and a pressure of 1 atm. It can be observed that the trend line of the predicted depth of corrosion values is in reasonable agreement with the trend line of the experimental depth of corrosion values. The average percentage error for the predicted depth of corrosion was -0.131% for the five test environmental conditions.

Table 6: Test environmental conditions given by numbers in Figure 14

No	pH	Applied load (N)	Time (days)
1	2.9	750	18
2	3.0	500	20
3	2.8	700	32
4	3.3	650	38
5	3.5	550	42

Limitation of the model

Although the model predicted values follow the upward and downward trends of experimental trend lines (Figure 9 and Figure 10), it can be seen that the model is predicting the lower depth of corrosion values under

some of the test environmental conditions, especially when the time duration approaches 30 days. Figure 9 shows that all the predicted depth of corrosion values from test environmental conditions 7 to 12 are less compared to the experimental depth of corrosion values. A similar trend is observed in Figure 10 as well.

The minimum depth of corrosion value, which was detected at the test environmental condition number 4 mentioned in Table 6, has a pH value of 3.5, applied load of 400 N and time duration of 15 days. However, this test environmental condition gives a minus value for the predicted depth of sulphide stress corrosion. However, the model starts showing a positive value for the depth of corrosion when the applied load reaches 408 N or higher values when the pH value is 3.5 and the time duration is 15 days. Therefore, the model gives an acceptable positive depth of corrosion values if the test environmental conditions are maintained under the following parameter ranges shown in Table 7.

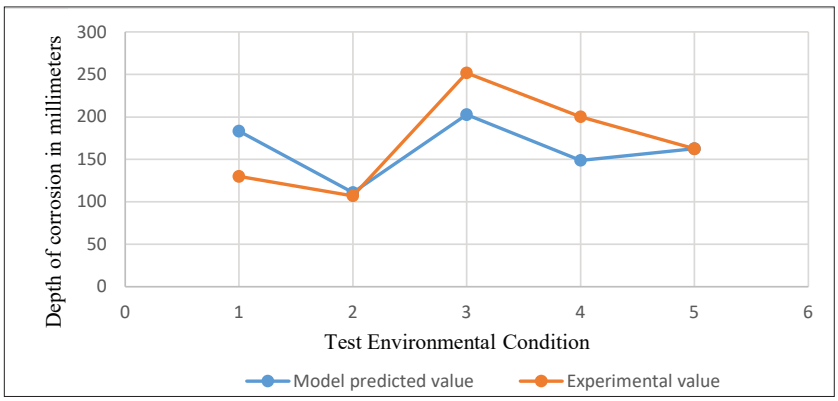

Figure 10: comparison between model prediction values and the experimental results

Table 7: Parameter ranges defined for the model at temperature 27 °C and pressure 1 atm

Parameter	Minimum value	Maximum value
Applied load	408 N	800 N
pH value	2.7	3.5
Time duration	15 days	45 days

Interpretation of behaviour of SSC by SEM/EDAX analysis

Experimental results indicated that the time period is the controlling factor in the initiation of cracks. Figure 11 shows the SEM image of a cross-section of the steel sample, which does not show crack initiation on the 14th day under test conditions of pH value 3.5 and applied load 600 N. According to Figure 12, it is obvious that the crack was initiated after 15 days under the same conditions. Therefore, at the primary stage, based on the experimental results, it was concluded that the initiation of cracks under all the aforementioned 18 sets of conditions occurs after an incubation period of 15 days, irrespective of the pH value and applied load.

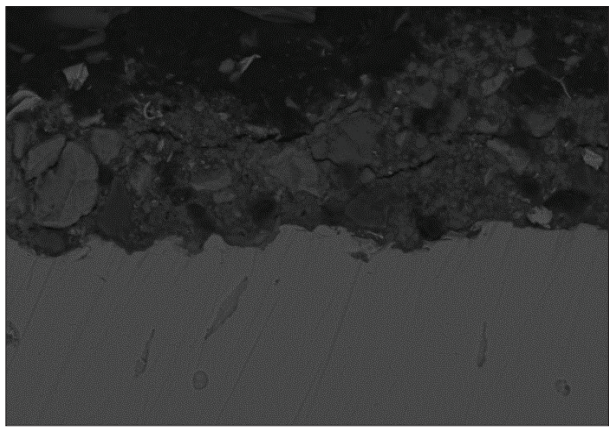

Figure 11: SEM image of the cross section of a specimen under the test conditions of pH value = 3.5, load = 600 N, time duration = 14 days

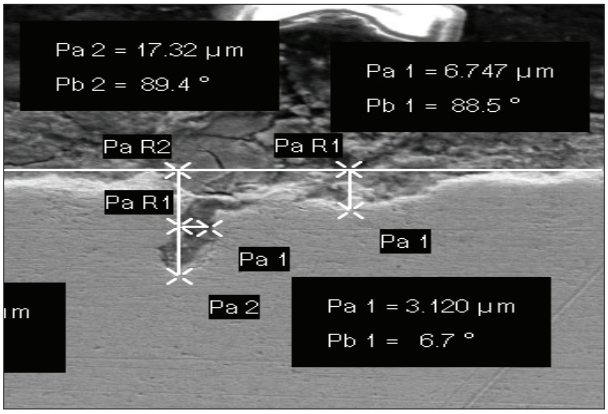

Figure 12: Sulphide stress crack initiation under the test conditions of pH value = 3.5, load = 600 N, time duration = 15 days

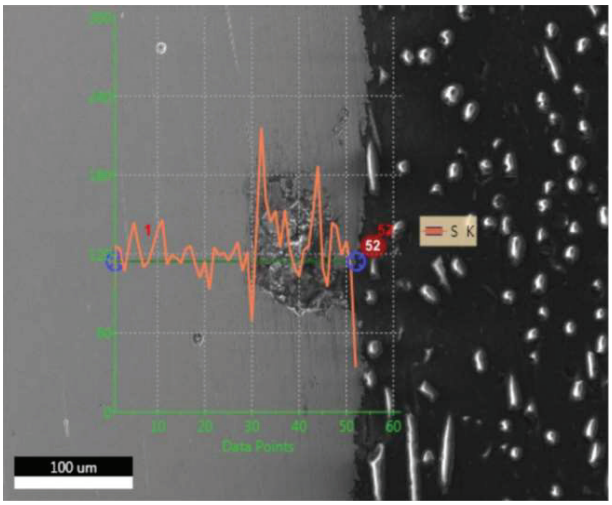

Figure 13: Elemental profile plot of the cross section of a specimen under the test conditions of pH value = 2.5, Load = 600 N, Time duration = 15 days

The initiation and propagation of sulphide stress cracks were investigated by SEM/EDAX analysis. The sulphur distribution along the crack was observed by SEM/EDAX elemental line profile, as shown in Fig 13, which clearly shows the higher content of sulphur associated with the crack relative to the other portions of the base metal. Therefore, these cracks can be identified as sulphide stress cracks.

The initiation of a sulphide stress crack occurs if there are surface discontinuities or surface pits (Ziaei *et al*., 2013). The formation of pits is a result of ruptures in the surface of mackinawite layers where the mackinawite is the predominant iron sulphide polymorph present in the corrosion product in the sour environment. Once the mackinawite layers reach a certain thickness, they rupture, leading to the formation of pits. These pits get filled with mackinawite with time (Smith, 2015). Later these pits grow into cracks (Smith, 2015). Once the initiation occurs, the crack starts to propagate transversely inwards to the core of the steel. The crack penetrates the steel, making branches similar to a growth of a taproot, as shown in Figure 14.

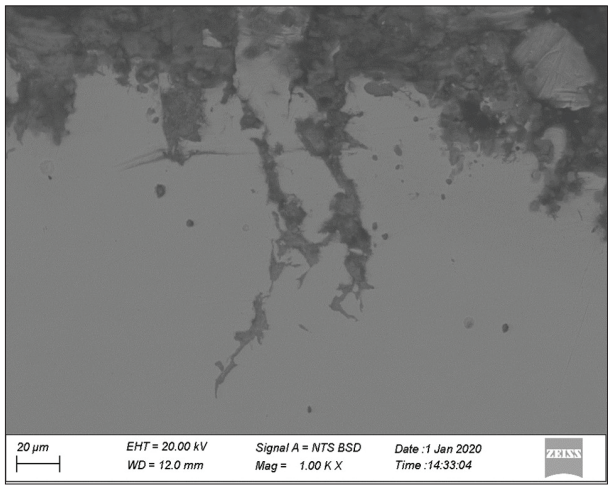

Figure 14: SEM image of the cross section of a specimen under the test conditions of pH value = 2.5, applied load = 400 N and time duration = 20 days

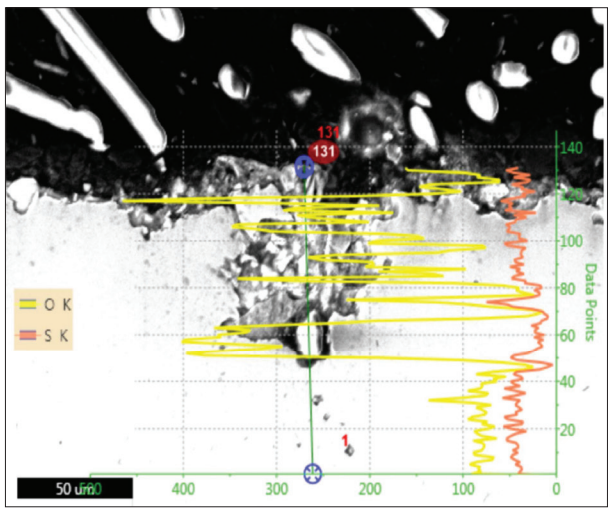

Figure 15: Elemental profile plot of the cross section of a specimen under the test conditions of pH value = 3.5, load = 600 N, time duration = 30 days

The SEM-EDAX elemental line profiles obtained for corroded samples in 30 days showed an interesting behaviour in the distribution of sulphur content throughout the crack. A sulphur-enriched area which was closer to the middle of the crack length, was observed (Figure 15). The formation of the sulphur-enriched area, specifically closer to the middle of the crack length relative to the crack initiation and tip areas, can be described based on the mechanism of the propagation of sulphide stress cracks.

In the sour environment, at high H_2S concentrations, mackinawite is the predominant component over iron carbonate in the corrosion layer. At low H_2S concentrations, both iron carbonate and mackinawite may be present in the corrosion product (Sun *et al*., 2008). Under both conditions, mackinawite forms very rapidly on the surface as a very thin, tightly adherent film (Smith, 2015). Mackinawite is formed through the direct heterogeneous reaction between S^{2-} and Fe^{2+} (Smith *et al*., 2002; Sun & Nesic, 2007; Cancio *et al*., 2012; Asmara *et al*., 2013). Once the mackinawite film is formed, it starts a reverse reaction to dissolve the formed mackinawite layers (Smith, 2015). If the formation rate of mackinawite is greater than the dissolution rate, the mackinawite layer begins to grow, covering the whole base metal. The continuous formation of the mackinawite layer causes multiple ruptures to form, and these ruptures act as pathways that allow the solution access to the mackinawite–based metal interface for continued corrosion via a tortuous path (Sun & Nesic., 2007; Cancio *et al*., 2012).

Mackinawite is an electron conductor (Pearce *et al*., 2006). The metal surface, which is underneath the mackinawite layer, dissolves, forming Fe^{2+}. The electrons removed from iron atoms are conducted through the mackinawite layer resulting cathodic reduction of hydrogen on the interlayer of mackinawite and the bulk solution. When the lattice parameters of the mackinawite crystal structure (Figure 16) are considered, the c dimension of the mackinawite crystal lattice is much larger than the a –b dimension (5.03 Å vs 3.67 Å). It forms an almost sheet-like structure. Because of this sheet-like structure, mackinawite can absorb divalent metallic cations into the lattice, as shown in Figure 17. Rather than substituting the cations for Fe^{2+} in the mackinawite structure, the adsorbed cations are moved between the "sheets" of iron sulphide (Zhao *et al*., 2005). Therefore, Fe^{2+} ions, which are formed at the anodic sites on the metal surface, should be able to migrate away from the metal surface towards the film-electrolyte boundary by moving along this path.

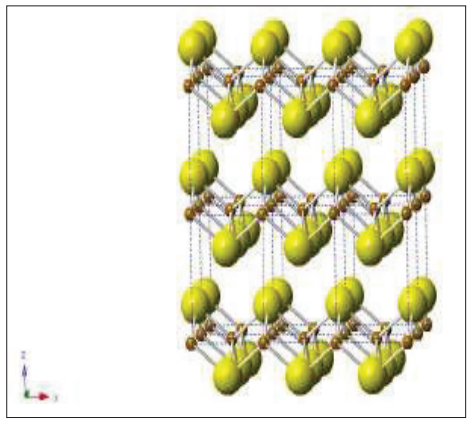

Figure 16: Mackinawite crystal structure

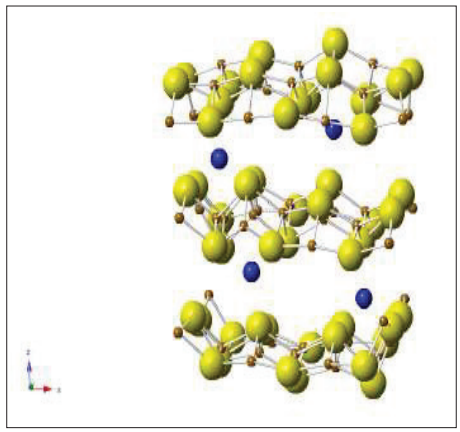

Figure 17: Mackinawite structure with additional cations (shown in blue color spheres) intercalated in the structure.

Fe^{2+} ions, which are formed on the metal surface, can find the film electrolyte along the ruptured pathways and within the interlayer of mackinawite - bulk solution. The Fe^{2+} ions which are diffusing out through the ruptured pathway can form FeS only along these ruptured pathways, and the Fe^{2+} ions which are moving along the planes of the mackinawite can form FeS once they meet a sudden ruptured pathway or once they meet the interlayer of bulk solution and the top surface of the mackinawite. When a cross-section of a crack is selected, much less mackinawite should be formed closer to the crack tip, and more mackinawite should be formed closer to the crack initiation point. Therefore, it can be expected that the ruptures along the crack length should be increased from crack initiation to crack tip. Similarly, the pathways

for the solution to enter the crack should be increased from crack initiation to crack tip. Therefore, when Fe^{2+} ions move upwards along the mackinawite sheets, there is a higher possibility of meeting more pathways of solution closer to the middle of the crack. Once they meet solution pathways, FeS is formed through direct heterogeneous reactions. Hence, the FeS-rich area can be seen closer to the middle of the crack (Figure 15).

CONCLUSION

The depth of sulphide stress corrosion of API 5L Grade B corresponding to the specific combination of pH value (2.7–3.5), applied load/pressure (400 N–800 N), and time duration (15 to 45 days) under ambient temperature and atmospheric pressure can be predicted using the developed model.

The results for the corrosion depths can be obtained through the model under the standard test conditions as per the ANSI/NACE TM0177-2016 standard test method.

Out of the aforementioned three major factors, it was found that the time duration is the leading factor that influences the crack initiation and propagation behaviour of sulphide stress corrosion.

Although the developed model successfully follows the experimental results, it underestimates the depth of sulphide stress corrosion when the time duration gets values closer to 30 days.

The propagation behaviour of sulphide stress corrosion can clearly be explained using SEM-EDAX elemental line profiles obtained for different directions of the propagated cracks. The observation of the formation of a sulphur-enriched area which was closer to the middle of the crack length, can be explained by relating the downward movement of the H_2S solution along the raptured pathways formed in the cracks and the upward movement of Fe^{2+} ions along the mackinawite sheets. Hence it can be concluded that the mackinawite formed as a corrosion product plays a dominant role in the propagation of sulphide stress corrosion.

Acknowledgement

The authors would like to express sincere appreciation to the Ceylon Petroleum Corporation for providing API 5L Grade B steel samples to conduct experiments. They also wish to thank the Senate Research Council (SRC) grant of the University of Moratuwa for providing financial assistance for the research project. The academic and non-academic staff of the Department of Materials Science and Engineering, University of Moratuwa are also acknowledged for their support in conducting laboratory experiments.

REFERENCES

American Petroleum Institute (2003). *Specification for Line Pipe*. American Petroleum Institute Washington DC, USA.

Asahi H., Ueno M. & Yonezawa T. (1994). Prediction of sulfide stress cracking in high-strength tubulars. *Corrosion* **50**(7): 537–545.
DOI: https://doi.org/10.5006/1.3294355

Asmara Y.P., Juliawati A., Sulaiman A. & Jamiluddin (2013). Mechanistic model of stress corrosion cracking (SCC) of carbon steel in acidic solution with presence of H_2S. *International Conference on Mechanical Engineering Research (ICMER2013)*, Bukit Gambang Resort City, Kuantan, Pahang, Malaysia.
DOI: https://doi.org/10.1088/1757-899X/50/1/012072

Cancio M.J., Latino M.L. & Perez T.E. (2012). Corrosion and hydrogen insertion in Uns G41300 steels in brine acid solutions saturated with hydrogen sulfide. *Corrosion 2012.* NACE-2012-1426, Salt Lake City, Utah.

European Commission (2013). *Corrosion-Related Accidents in Petroleum Refineries.* Publications Office of the European Union, Luxembourg.

Foroulis Z.A. (1996). The mechanism of refinery corrosion by sour water condensates. *Anti-Corrosion Methods and Materials* **29**(3): 4–14.
DOI: https://doi.org/10.1108/eb007188

Gossett J. (2007). Detecting sulfide stress cracking and applying NACE MR0175. *Today's Refinery* **80921**: 1–14.

Liao K., Yao Q., Wu X. & Jia W.A. (2012). Numerical corrosion rate prediction method for direct assessment of wet gas gathering pipelines internal corrosion. *Energies* **5**(10): 3892–3907.
DOI: https://doi.org/10.3390/en5103892

NACE international standard (2005). *Standard Test Method Laboratory Testing of Metals For Resistance to Sulfide Stress Cracking and Stress Corrosion Cracking in H_2S Environments*. Houston, Texas, USA.

Pearce C.I., Patrick R.A.D. & David J.V. (2006). Electrical and magnetic properties of sulfides. *Reviews in Mineralogy and Geochemistry* **61**: 127–180.
DOI: https://doi.org/10.2138/rmg.2006.61.3

Peiris M.D.H.C., Perera W.L. & De Silva G.I.P. (2020). Study of the effect of sulphide stress corrosion on the load bearing capability of API 5L Grade B steel used in petroleum pipelines. *Engineer: Journal of the Institution of Engineers* **53**(2): 13–21.
DOI: https://doi.org/10.4038/engineer.v53i2.7408

Smith S.N., Jorge L. & Pacheco (2002). Predicting corrosion in slightly sour environment. *Corrosion 2002,* Denver, Colorado, USA.

Smith S.N. (2015). Current understanding of corrosion

mechanisms due to H_2S in oil and gas production environments. *NACE - International Corrosion Conference Series.* Woodlands, Texas, USA.

Statistics Solution (2016). Available at *http://www.statisticssolutions.com*. Accessed 2020.

Sun W. & Nesic S. (2007). A mechanistic model of H_2S corrosion of mild steel. *Corrosion 2007 Conference and Expo*, Athens, Ohio, USA.

Sun W., Nesic S. & Papavinasam S. (2008). Kinetics of corrosion layer formation, Part 2 – iron sulfide and mixed iron sulfide/carbonate layers *Corrosion* **7**(64): 586–599. DOI: https://doi.org/10.5006/1.3278494

Traidia A., Chatzidouros E. & Jouiad M. (2018). Review of hydrogen-assisted cracking models for application to service lifetime prediction and challenges in the oil and gas industry. *De Gruyter* **36**(4): 323–347. DOI: https://doi.org/10.1515/corrrev-2017-0079

Zhao J.M., Wei Z., Zuo Y. & Zhao X.H. (2005). Effects of some ions on ion-selectivity of ferrous sulfide film. *Journal of Applied Electrochemistry.* **35**: 267–271. DOI: https://doi.org/10.1007/s10800-004-6704-8

Zheng Y., Ning J., Brown B. & Nesic S. (2014). Electrochemical model of mild steel corrosion in a mixed h2s/co2 aqueous environment. *Corrosion* **3901**: 1–20.

Ziaei S.M.R., Kokabi A.H. & Nasr-Esfehani M. (2013). Sulfide stress corrosion cracking and hydrogen induced cracking of A216-WCC wellhead flow control valve body. *Case Studies in Engineering Failure Analysis* **1**(3): 223–234. DOI: https://doi.org/10.1016/j.csefa.2013.08.001